Available online at www.sciencedirect.com
ScienceDirect
Geochimica et Cosmochimica Acta 71 (2007) 1721–1736
Geochimica et Cosmochimica Acta
www.elsevier.com/locate/gca

A radical pathway for organic phosphorylation during schreibersite corrosion with implications for the origin of life

Matthew A. Pasek [a,*], Jason P. Dworkin [b], Dante S. Lauretta [c]

[a] *Steward Observatory, 1629 E. University Blvd, University of Arizona, Tucson, AZ 85721, USA*
[b] *Astrochemistry Branch, NASA Goddard Space Flight Center, Greenbelt, MD, USA*
[c] *Lunar and Planetary Laboratory, University of Arizona, Tucson, AZ, USA*

Received 29 August 2006; accepted in revised form 23 December 2006; available online 10 January 2007

Abstract

Phosphorylated compounds (e.g., DNA, RNA, phospholipids, and many coenzymes) are critical to biochemistry. Thus, their origin is of prime interest to origin of life studies. The corrosion of the meteoritic mineral schreibersite ($(Fe,Ni)_3P$) may have significantly contributed to the origin of phosphorylated biomolecules. Corrosion of synthetic schreibersite in a variety of solutions was analyzed by nuclear magnetic resonance spectroscopy, mass spectrometry, and electron paramagnetic resonance spectroscopy. These methods suggest a free-radical reaction pathway for the corrosion of schreibersite to form phosphite radicals ($\cdot PO_3^{2-}$) in aqueous solution. These radicals can form activated polyphosphates and can phosphorylate organic compounds such as acetate to form phosphonates and organophosphates (3% total yield). Phosphonates (O_3P–C) are found in the organic P inventory of the carbonaceous meteorite Murchison. While phosphonates are rare in biochemistry, the ubiquity of corroding iron meteorites on the early Earth could have provided a source of organic phosphorous compounds for the origin of life, and may have led to the role of organophosphates as a product of early evolution.

1. INTRODUCTION

Determining the origin of phosphorylated biomolecules is a central goal of origins of life research. Phosphorylated biomolecules are critical components of life important for structure (phospholipids), information (DNA), and energetics (e.g., ATP, UDPG). In contrast to the active role of P in life, phosphate minerals are sparingly soluble in water and lack reactivity towards most organic molecules. The formation of phosphorylated biomolecules is inhibited by the geochemistry of P on the Earth and many scenarios for the origin of phosphorylated biomolecules have employed unlikely geochemical settings (e.g., Keefe and Miller, 1995; Peyser and Ferris, 2001). Following the discovery of phosphonic acids in the Murchison carbonaceous chondrite, some researchers have proposed that extraterrestrial material may have provided the initial reactive and soluble phosphorus for life (e.g., de Graaf et al., 1995; Macià et al., 1997).

The meteoritic mineral schreibersite, $(Fe,Ni)_3P$, is a proposed source of reactive P for the origin of phosphorylated biomolecules (Gulick, 1955; Pasek and Lauretta, 2005; Bryant and Kee, 2006). Schreibersite readily corrodes in aqueous solution to form a mixed-valence series of P compounds, including orthophosphate (I, oxidation state +5), pyrophosphate (II, oxidation state +5), phosphite (III, oxidation state +3), hypophosphate (IV, oxidation state +4), and, under some conditions, diphosphite (V, oxidation state +3) (Fig. 1).[1] These compounds are produced independent of the atmospheric composition above these solutions (Ar or air), differing only in total yield. In the presence of acetate/ethanol several organophosphorus compounds are also formed (Pasek and Lauretta, 2005).

* Corresponding author. Fax: +1 520 621 9692.
E-mail address: Mpasek@lpl.arizona.edu (M.A. Pasek).

[1] Using the nomenclature of Van Wazer (1958) for the salts.

0016-7037/$ - see front matter © 2007 Elsevier Ltd. All rights reserved.
doi:10.1016/j.gca.2006.12.018

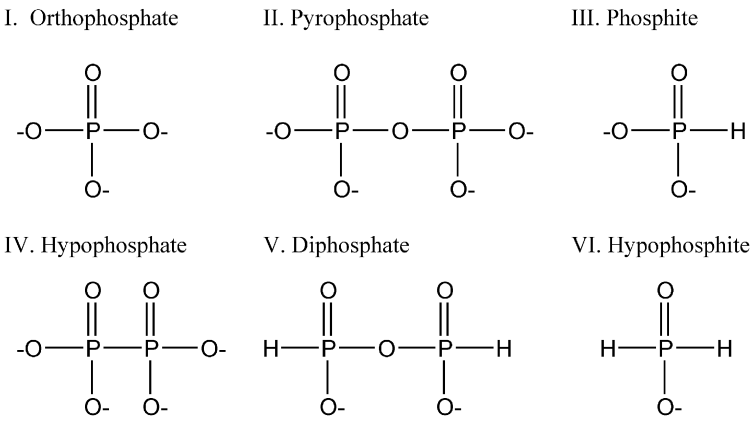

Fig. 1. Inorganic phosphorus compounds discussed in text. Bryant and Kee (2006) identified I–IV, and produced VI under UV light.

A better understanding of the reaction is critical to an evaluation of the prebiotic input of schreibersite to the origin of life, and to the origin of the P–C molecules in the organic inventory of meteorites. The complexity of the solution chemistry of corroding schreibersite implies the activity of several reactions. We propose a reaction pathway that is consistent with the nuclear magnetic resonance (NMR), mass spectrometry (MS), electron paramagnetic resonance (EPR), and analogy with other reactions. The reaction pathway consists of a series of radical reactions culminating in a series of P salts, and that radical chemistry overcomes energy barriers traditionally associated with the phosphorylation of organics.

Two groups of experiments were performed to investigate the process of P speciation from phosphide corrosion. One set of experiments examined the effect of aqueous corrosion of iron phosphide, Fe_3P, on a suite of simple compounds (Experiments 1–22, Table 1). A majority of these experiments were performed under air to maximize yield for analysis. Though experiments performed under air can not be assumed to represent the prebiotic environment, results suggested little qualitative difference in P speciation between experiments performed in air or argon. The primary difference between air and Ar was total yield. Experiments performed under air were about a factor of ten more concentrated and hence were easier to characterize. A second set of experiments (23–32) investigated the stability and reactivity of phosphite, orthophosphate, hypophosphate, and pyrophosphate in the presence or absence of corroding metal; compounds produced during schreibersite corrosion. The stability of hypophosphite (oxidation state +1, Fig. 1, VI) was also investigated as this compound is a plausible reaction intermediate.

2. MATERIALS AND METHODS

2.1. Materials and conditions

Phosphide was introduced as pure Fe_3P powder (−40 mesh, purchased from CERAC, Inc.). High-purity iron powder (99+%, Alfa Aesar) was used in some of the corrosion experiments. Magnetite was from Serro, Minas Gerais, Brazil. The solution volume for all experiments was 25 mL. Aqueous solutions were either pure deionized water, purified in house using a Barnstead NANOpure® Diamond Analytical combined reverse osmosis-deionization system, or were solutions created by adding compounds to the deionized water. Solutions were from salts of Mg- and Ca-chloride (98%, from Alfa Aesar), reagent alcohol (90.5% ethanol, 5% isopropanol, and 4.5% methanol from VWR lab supplies), acetic acid (99.7% from EMD lab supplies), $NaHCO_3$ (Arm and Hammer, 99+%), glycolaldehyde (MP Biomedicals LLC., 99+%), acetaldehyde (Merck, 99+%), ethylenediaminetetraacetic acid (from VWR lab supplies), H_2O_2 (30% in water, VWR lab supplies), pyruvate (Alfa Aesar, 98%), acetonitrile (J.T. Baker, 99.8%), 5-5-dimethyl-1-pyrroline-*N*-oxide (DMPO from Alexis Biochemicals, 100%, stored at −10 °C) or a combination of these components. The pH was between 6.5 and 8 in most experiments with the reported pH determined by a Hach SensIon 156 pHmeter before and after reaction. The pH of the buffer was adjusted using NaOH (from VWR, 10.0 N stock solution) or NH_4OH (from ADChemco Scientific Inc., 28–30% in water). Half of each solution was isolated from the phosphide and saved for comparison as a blank.

Pure compounds were used as standards for species identification and were prepared at 0.01 M in D_2O and NaOH (pH 13). Standards used include H_3PO_3, H_3PO_4, $Na_4P_2O_7$, NaH_2PO_2, $C_2H_5PO_3H_2$, $CH_3PO_3H_2$, $(CH_3)_3PO_4$, $Ba(PO_3)_2$, and P_2O_5 and were acquired from VWR International, and acetylphosphonic acid ($H_2O_3PCH_2COOH$, 98+%) was acquired from Alfa Aesar. Hypophosphate was synthesized by the method of Yoza and Ohashi (1965) and verified by ^{31}P NMR. The temperature in all experiments was ~20 ± 3 °C measured in situ using a mercury thermometer. The Ar (99.99%) was from University of Arizona Laboratory Stores.

2.2. Experimental setup

Experiments were mostly performed under ambient atmospheric conditions (NMR Air) with some under argon to remove most dissolved O_2 from the water as well as to maintain an inert atmosphere prior to introduction of the phosphide to the water (note that Ar is prepared from

Table 1
Experiments reported in this work

No.	Method(s)	Solution	Solid (mass in g)	pH
1	NMR Air[a]	Water	Fe_3P (1.0473 g)	7
2	NMR Air[a]	$MgCl_2/CaCl_2$ (0.025 M)	Fe_3P (1.4100 g)	7
3	NMR Air[a]	CH_3COONa (0.4 M), EtOH (0.4 M)	Fe_3P (1.1347 g)	6.5
4	NMR Air[a]	$MgCl_2/CaCl_2$ (0.04 M),CH_3COONa (0.2 M), EtOH (0.2 M)	Fe_3P (1.0368 g)	6.5
5	NMR Air[a]	$NaHCO_3$ (0.5 M)	Fe_3P (0.6941 g)	9.5
6	NMR Air	NaCl (0.4 M)	Fe_3P (0.9811 g)	7
7	NMR Air	NaOH (0.05 M), EDTA (0.025 M)	Fe_3P (1.0686 g)	13
8	NMR Air	CH_3CN (0.4 M)	Fe_3P (1.0765 g)	7
9	NMR Air	EtOH (0.4 M)	Fe_3P (0.8216 g)	7
10	NMR Air	Acetone (0.4 M)	Fe_3P (0.9636 g)	7
11	NMR Air	CH_3COONa (0.4 M)	Fe_3P (0.7378 g)	6.5
12	NMR Air	Pyruvate, $C_3H_3O_3Na$ (0.7 M)	Fe_3P (0.8421 g)	6
13	NMR Air	Acetaldehyde, CH_3CHO (1.2 M)	Fe_3P (0.8212 g)	7
14	NMR Air	H_2O_2 (0.6 M)	Fe_3P (1.3313 g)	7
15	NMR Argon[a]	Water	Fe_3P (1.2197 g)	7
16	NMR Argon[a]	$MgCl_2/CaCl_2$	Fe_3P (1.0325 g)	7
17	NMR Argon[a]	CH_3COONa (0.4 M), EtOH (0.4 M)	Fe_3P (1.1629 g)	6.5
18	NMR Argon[a]	$NaHCO_3$ (0.5 M)	Fe_3P (1.3208 g)	9.5
19	NMR Argon	Glycolaldehyde, $C_2H_4O_2$ (0.4 M)	Fe_3P (0.9848 g)	7
20	ES-TOF-HR-MS Air	CH_3COONH_4 (0.4 M)	Fe_3P (0.9857 g)	8
21	ESR Air	NaOH (0.1 M), DMPO (0.2 M)	Fe (~1 g)	13
22	ESR Air	DMPO (0.2 M)	Fe_3P (~1 g)	7
23	NMR Air[a]	Na_2HPO_3 (0.01 M)	Fe (0.7158 g)	7
24	NMR Air[a]	Na_2HPO_3 (0.01 M)	—	7
25	NMR Air[a]	Na_2HPO_3 (0.03 M)	Fe_3O_4 (0.5912 g)	7
26	NMR Air[a]	NaH_2PO_2 (0.05 M)	Fe (0.6758 g)	7
27	NMR Air[a]	NaH_2PO_2 (0.05 M)	—	7
28	NMR Air	NaH_2PO_2 (0.08 M), Na_2HPO_3 (0.03 M)	—	7
29	NMR Air	NaH_2PO_2 (0.08 M), Na_2HPO_3 (0.03 M)	Fe_3O_4(0.6500 g)	7
30	NMR Air	Na_2HPO_4 (0.5 M)	Fe (~0.5 g)	7
31	NMR Air	$Na_4P_2O_6$ (0.05 M)	Fe (1.0721 g)	13
32	NMR Air	$Na_4P_2O_7$ (0.5 M)	Fe (~0.5 g)	13

NMR is nuclear magnetic resonance spectrometry, ES- TOF-HR-MS is negative electron spray time of flight-high resolution-mass spectrometry, ESR is electron spin resonance spectrometry. More details can be found in Pasek (2006).
[a] Data presented in Pasek and Lauretta (2005). Included here for completeness.

fractional distillation from air, and thus Ar gas will have some O_2 as this is unavoidable). The corrosion of phosphide under Ar (Pasek and Lauretta, 2005) and N_2, (Bryant and Kee, 2006) generates the same products but at lower concentration than under air thus several of these experiments were performed under air to maximize detection.

Solutions of 0.01–0.5 M P compound were used for the stability experiments. These solutions were sealed with or without ~0.5–1 g of Fe powder or ~0.5 g of crushed magnetite. Samples were analyzed after one day of constant stirring.

NMR analysis was at pH 13 as the addition of NaOH sharpens NMR peaks and allow for comparison with previous studies. The carbonate solutions were analyzed at a pH 9.5 since a large volume of NaOH is required to overpower the buffer. The samples were filtered, the extract concentrated by vacuum and then redissolved in 5 mL of D_2O (99.7%, Alfa Aesar).

One experiment replicated the phosphide corrosion in acetic acid under air with NH_4OH instead of NaOH. This allowed analysis by ES^- ToF-MS (negative Electrospray Time of Flight Mass Spectrometry) to avoid sodium acetate clusters. Prior to analysis, the sample was dried under vacuum to remove NH_3. The remaining material had a slight red coloration.

Corrosion experiments analyzed by Electron Paramagnetic Resonance (EPR) spectrometry were prepared by removing a small quantity of solution and adding the spin trap DMPO (0.2 M final concentration). It is necessary to employ a radical spin trap as phosphite radicals are too short-lived to be detected in aqueous solution (Ozawa and Hanaki, 1987). No NaOH was added to the phosphide sample and no metal grains were transferred to the DMPO analysis.

2.3. Analytical methods

Each solution was analyzed using ^{31}P NMR on a Varian 300 four-nucleus probe FT-NMR (Fourier Transform-NMR) spectrometer at 121.43 MHz and 24.5 °C for 256–35,000 scans. Spectra were acquired in both H-decoupled and coupled modes.

The bulk dissolved P content was measured for five solutions using a ThermoFinnigan ELEMENT2 high-resolution Inductively Coupled Plasma Mass Spectrometer (ICP-MS). Analytical details are in Pasek and Lauretta

(2005). The ICP-MS data ($R^2 = 0.9939$) were used to calibrate the NMR to determine P molarity $[M]$ in solution by the the following equation:

$$[M] = 0.0075 \times \left(\frac{\left(\frac{S}{N}\right)}{\sqrt{\text{Scans}}}\right)^2 + 0.0007 \times \left(\frac{\left(\frac{S}{N}\right)}{\sqrt{\text{Scans}}}\right) + 0.0001, \quad (1)$$

where S is the signal, N is the noise, and Scans is the number of NMR scans taken. This relationship was empirically determined and is accurate to ~10% over the range of 10^{-4} to 10^{-2} M based on the sample spectra acquired.

The concentration of each P compound was determined by integration of the NMR spectrum. NMR integration is quantitative if the integration is done over a narrow range of frequencies, typically less than 50 ppm. Turning the H-decoupler off during NMR acquisition had no effect on integrations compared with acquisitions with the H-decoupler on, indicating that the Nuclear Overhauser Effect (NOE) did not affect integrations significantly.

Mass spectrometry was performed by infusing a solution into a Waters LCT Premier Time of Flight Mass Spectrometer (TOF-MS) at 100 μL/min. Soft ionization was performed with ES^- with 4200 V capillary voltage, 300 °C desolvation gas temperature, and 10 V cone voltage. The MS was in "W" reflectron mode with a mass resolution of <3 ppm and scanned over 50–400 m/z. The mass calibration was performed continuously using adenine ($-H^+$) (M/Z = 134.0467 Da) every 10 scans via a dedicated sprayer. Minimal ionization was observed in ES^+ mode. A spectrum was acquired every second for 3 min after which time the spectra were summed and averaged. The relative concentrations of the four species $H_2PO_3^-$, $H_2PO_4^-$, $H_3P_2O_6^-$, and $H_3P_2O_7^-$ were determined by NMR and used to estimate the concentrations of other species detected by the MS. Differences in ionization efficiency result in large uncertainties (~a factor of 2).

EPR analyses were performed using a continuous wave X-band (9–10 GHz) EPR spectrometer, model ESP-300E manufactured by Bruker. Samples were siphoned into capillary tubes and analyzed with a 1 Gauss modulation and a 20 mW microwave power source. Each spectrum consists of 30 scans from 3290–3390 Gauss.

3. RESULTS

In all experiments exposed to air the phosphide powder changed color from gray to a reddish brown. In the experiments isolated from air and flushed under argon, color change was limited to black. Some organic corrosion experiments turned to a mixture of iron rust and tar which we were not able to analyze. The pH of all systems remained relatively unchanged (pH changes <0.5). We identified a number of P species in aqueous solution. The concentrations of all P species and total concentration of P in Experiments 1–19 is given in Table 2. The inorganic ionic species were identified based on comparison to standards and literature values (Yoza et al., 1994). One organic P compound, acetyl phosphonate, was positively identified by comparison to a prepared standard. Others were identified through literature comparisons.

The total yields of dissolved P compounds relative to the amount of phosphide material employed in corrosion range from 0.1% to 10%. The two major factors affecting yield are solution chemistry and atmosphere composition where solution chemistry appears to have a larger effect.

3.1. NMR experiment results

Table 3 summarizes the coupling constants, peak locations, and other pertinent NMR data from the experiments detailed below, including detection of organophosphorus compounds that were identified using data from the ES^- ToF-MS.

For Experiments 1–19, analyses of blank solutions by NMR revealed no detectable P contamination. All P observed by NMR in solution originated from the corroded phosphide Nearly all experiments had four major ^{31}P NMR peaks (hypophosphate, orthophosphate, phosphite, pyrophosphate, Table 2). The most diverse P chemistry occurred in organic solution corrosion.

The experiments with acetone and with glycolaldehyde both formed a rust-colored tar which could not be analyzed by conventional NMR. Experiments with ethanol or acetonitrile aqueous solutions produced no new products. Acetate and to a lesser extent other carbonyls (pyruvate, acetaldehyde, and EDTA) generated a diverse suite of soluble products without polymerizing into tar. Experiment 4 corroded Fe_3P in a solution of Mg and Ca salts with acetate and ethanol. This experiment produced mainly phosphite in solution.

The iron phosphide powder was also corroded in a H_2O_2 solution (Experiment 14). The products detected by NMR were surprisingly similar those generated from acetate (Fig. 2), the major exception is the presence of minor organophosphorus species in the acetate experiment.

3.2. Mass spectral experiments

Mass spectral analysis of the CH_3COONH_4 and Fe_3P experiment (#20) indicates that a large variety of P compounds were produced during this corrosion experiment (Fig. 3). Plausible identifications of these compounds are summarized in Table 4.

The mass resolution (< 3 ppm) allows the determination of molecular formulas for the detected species. Several mass peaks correspond well with compounds known from the NMR analysis, including phosphite ($H_2PO_3^-$), orthophosphate ($H_2PO_4^-$), hypophosphate ($H_3P_2O_6^-$), pyrophosphate ($H_3P_2O_7^-$), and diphosphite ($H_3P_2O_5^-$).

3.3. Electron paramagnetic resonance spectrometry analyses

Samples of Fe and Fe_3P were corroded in deionized water to determine the nature and concentration of radicals in solution. Fig. 4 shows the EPR spectra from DMPO and water (background), DMPO and Fe in basic solution, and DMPO and Fe_3P in neutral water. No peaks are observed in the background spectrum, indicating that the diradical

Table 2
Results of corrosion experiments

No.	Atmo	Solution	Bulk P in mM	Pi (μM)	P3 (μM)	P4 (μM)	PPi (μM)	Other μM (Identification)
1	Air	Water	2.30	430	1100	360	450	
2	Air	$MgCl_2/CaCl_2$	1.07		1100			
3	Air	CH_3COONa, EtOH	9.49	3000	4200	1300	140	1610 (Many)
4	Air	$MgCl_2/CaCl_2$, CH_3COONa, EtOH	0.368		370			Minor P–O–C ?
5	Air	$NaHCO_3$	14.7	6700	2700	620	2900	1800 (Diphosphite)
6	Air	NaCl	5.2	930	2500	750	700	
7	Air	NaOH, EDTA	3.8	1300	1600	460	430	26 (P–H compounds)
8	Air	CH_3CN	6.4	1700	3500	770	470	
9	Air	EtOH	0.89	420	340	91	44	
10	Air	Acetone	ND				Turned to tar	
11	Air	CH_3COONa	11.7	5400	4000	790	120	1400 (Many)
12	Air	Pyruvate	0.66	170	240	68	50	140 (Many)
13	Air	Acetaldehyde	0.40	180	120	110	29	Trace (Many)
14	Air	H_2O_2	5.3	2800	1600	750	250	35 (Many)
15	Argon	Water	0.269	130	100	18	23	
16	Argon	$MgCl_2/CaCl_2$	0.27		270			
17	Argon	CH_3COONa, EtOH	3.1	940	1300	340	510	80 (Many)
18	Argon	$NaHCO_3$	0.33	120	130	22	44	22 (Diphosphite)
19	Argon	Glycolaldehyde	ND				Turned to tar	

P compounds given in μM. Pi is orthophosphate, P3 is phosphite, P4 is hypophosphate, and PPi is pyrophosphate. ''Other'' includes a number of varied species with definite identifications listed. Errors are ~1% for ICP-MS and ~10% for NMR.

Table 3
NMR peak location data, pH of 13

Compound ID	Peak (ppm)	Coupling constant
Deionized water and Saline Experiments		
Hypophosphate	14.4264	
Orthophosphate	6.42304	
Phosphite	4.17083	1 bond P–H (570 Hz)
Pyrophosphate	−3.52734	
Acetate Experiment (in addition to the peaks above)		
Unknown P compound	37.7126	
Unknown P compound	37.3909	1 bond P–P (308 Hz),
Unknown P compound	34.8571	2 bond P–P (40 Hz)
Unknown P compound	34.5736	
P–H compound[a]	26.6125	1 bond P–H (449 Hz)
P–H compound[a]	22.7918	1 bond P–H (444 Hz)
Methyl Diphosphite	19.4	?
Unknown organic P compound	17.8	2 bond P–H (72 Hz)
Acetyl phosphonate	15.593	2 bond P–H (30 Hz)
Unknown organic P compound	12.7775	
Hydroxylmethyl phosphonate	11.8927	2 bond P–H (20 Hz)
Unknown organic P compound	11.3296	
Unknown P compound[a]	9.31873	
Unknown P compound[a]	9.19808	
Phosphoglycolate?	3.4	3 bond P–H (18 Hz)
Phosphonoformate?	−0.8	
Diphosphite[a]		1 bond P–H (650 Hz),
	−2.726	3 bond P–H (20 Hz)
Other condensed phosphates	−9.3424	
Other condensed phosphates	−10.7903	
Other condensed phosphates	−17.5871	
Other condensed phosphates	−19.2763	

[a] Also in H_2O_2 experimental corrosion.

O_2 from air is not trapped as a radical species to any significant observable extent. The peaks shown in Figs. 4b and c confirm the presence of radical species in solution.

The EPR spectrum of DMPO and Fe (Fig. 4b) in basic solution corresponds well to literature spectra of the radical DMPOOH (Sankarapandi and Zweier, 1999) which is formed by reaction of DMPO with ·OH radicals. The EPR spectrum of DMPO and Fe_3P (Fig. 4c) corresponds to a mixture of DMPOOH and DMPOX (oxidized DMPO) radicals in a 5:3 ratio. DMPOX radicals are formed from the interaction of $\cdot PO_3^{2-}$ radicals with DMPO (Ozawa and Hanaki, 1989).

3.4. Organic phosphorus compounds formed

Plausible structures of identified compounds are shown in Fig. 5.

The masses and total concentrations of each organic P compound are listed in Table 4. Chemical shifts of methyl diphosphite, acetyl phosphonate, and hydroxylmethyl phosphonate are consistent with published spectra as are the *J*-couplings for these compounds (Satre et al., 1989; Robitaille et al., 1991; Noguchi et al., 2004) and these identifications are confirmed by the MS analysis. In addition, the acetyl phosphonate peak matched well when compared to an NMR standard of this compound. Phosphoglycolate may be present in solution but its peak would be overcome by the much stronger phosphite peak in Fig. 2b. Phosphonoformate has an NMR peak of between −1 and 1 ppm, depending on pH and may be observed in Fig. 2b in this area.

Pasek and Lauretta (2005) discuss the possible presence of a cyclic organic P compound. The present data set does not support the presence of this compound, as the Fe_3P and H_2O_2 experiment produced peaks identical to those of the purported organic P compound, despite the lack of any added organics. Cyclic organic P compounds may have been detected by MS, but several of these putative identifications are isomeric with non-cyclic P compounds, hence they have not been included in Table 4.

3.5. P compound stability experiments

The motivation for this set of experiments was to understand the stability and reactivity of P species in the presence of metal. Results are presented in Table 5. Hypophosphite ($H_2PO_2^-$) is a plausible intermediate in oxidation state between Fe_3P and HPO_3^{2-}. It does not appear in any of the above corrosion experiments, but it may serve as a short-lived reactive intermediate. We determined its stability through monitoring this compound over the course of one day. After one day, ~25% of hypophosphite is converted to phosphite under air, independent of material added to the solution (no addition; Fe added; Fe_3O_4 added).

Phosphite is more stable than hypophosphite over longer periods of time, with no conversion to other P

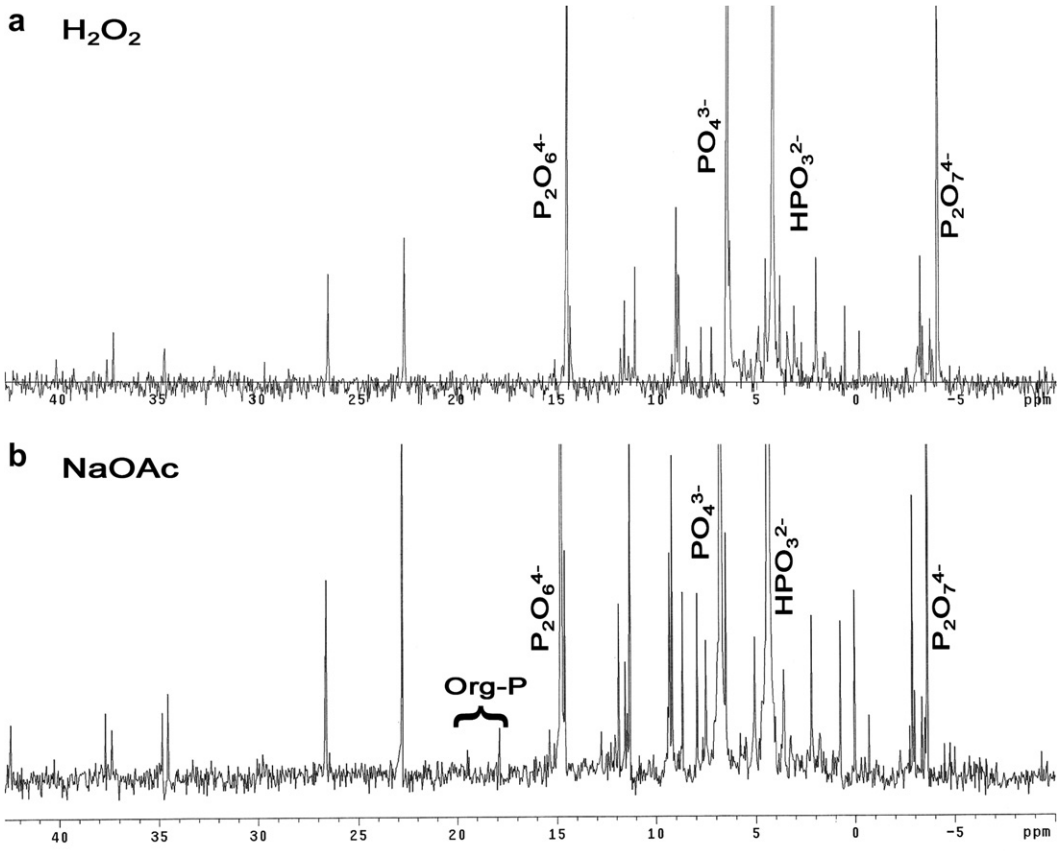

Fig. 2. A comparison of NMR spectra. (a) Fe_3P with H_2O_2 (0.6 M) and (b) Fe_3P with sodium acetate ± ethanol (0.4 M). The peak heights of both spectra have been increased substantially to allow for comparison between solutions. Major peaks are inorganic P oxides and are identified. Note the organic P compounds present between 15 and 20 ppm in (b).

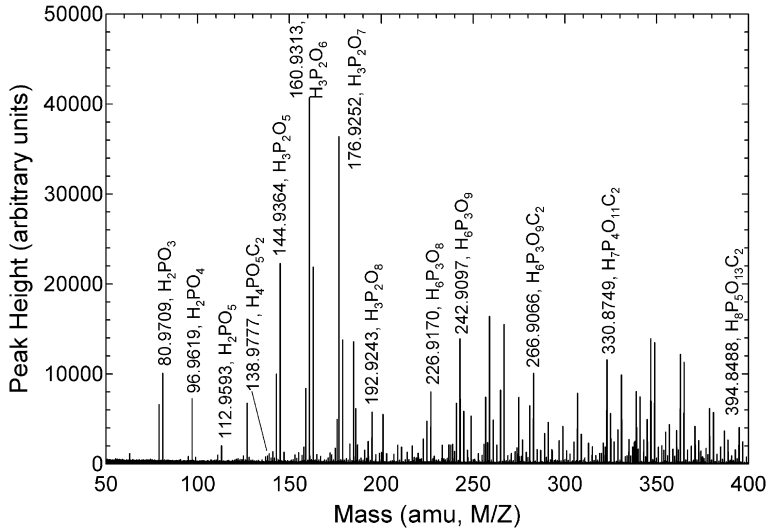

Fig. 3. Mass spectrum of NH_4OOCCH_3 and Fe_3P corrosion solution. The tallest peaks are labeled and identified. Note that concentration is proportional to peak height and total mass and that the concentrations in Table 4 were determined by standardizing the peak heights to known NMR concentrations.

compounds under ambient conditions. Addition of Fe metal to the solution results in a conversion of ~46% of phosphite to orthophosphate in one day. Addition of magnetite has no effect and the phosphite concentration was unchanged.

Experiments with orthophosphate, hypophosphate, and pyrophosphate added to Fe metal did not change significantly with time. Experiments substituting Fe_3P powder for Fe metal produced identical results (Pasek, 2006). No

Table 4
Mass spectral peaks observed in the aqueous reaction of NH_4OOCCH_3 and Fe_3P

Mass	ID	Concentration (μM)	Note
80.9709	H_2PO_3	5300	NMR
78.9563	PO_3	3700	H_2
96.9619	H_2PO_4	2200	NMR
160.9313	$H_3P_2O_6$	1500	NMR
144.9364	$H_3P_2O_5$	1400	NMR
62.9643	PO_2	1100	H_2
176.9252	$H_3P_2O_7$	790	NMR
126.9275	HP_2O_4	770	H_2?
162.9478	$H_5P_2O_6$	750	H_2
142.9206	HP_2O_5	670	H_2
112.9593	H_2PO_5	370	NMR?
158.9191	HP_2O_6	330	H_2
178.9419	$H_5P_2O_7$	280	H_2
184.9285	$H_3P_2O_6C_2$	230	H_2?, Org?
110.9894	H_4PO_4C	190	NMR, Hydroxylmethyl phophonate
175.9416	?	110	
140.9343	$H_4P_3O_2C$	100	H_2?, Org?
124.9642	H_2PO_5C	90	NMR?, Phosphonoformic acid
138.9777	$H_4PO_5C_2$	80	NMR, Acetylphosphonate
157.9327	?	80	
194.936	$H_5P_2O_8$	70	H_2
154.9842	$H_4PO_6C_2$	60	NMR?, Phosphoglycolate
200.9222	$H_3P_2O_7C_2$	50	H_2?, Org?
153.0081	$H_6PO_5C_3$	50	Org
174.9456	$H_5P_2O_6C$	40	NMR, Methyl diphosphite
182.9121	$HP_2O_6C_2$	40	H_2?, Org?
242.9097	$H_6P_3O_9$	30	H_2
226.917	$H_6P_3O_8$	30	H_2
192.9243	$H_3P_2O_8$	30	
258.9053	?	20	
224.8996	$H_4P_3O_8$	20	NMR?
190.9515	$H_5P_2O_7C$	25	Phosphonomethylphosphate
240.8961	$H_4P_3O_9$	20	
266.9066	$H_6P_3O_9C_2$	20	Tri-P-acetate
208.9235	$H_4P_3O_7$	20	
202.936	$H_5P_2O_7C_2$	16	Hypophosphatoacetate
330.8749	$H_7P_4O_{11}C_2$	7	Quad-P-acetate
394.8488	$H_8P_5O_{13}C_2$	1	Penta-P-acetate

Concentration is compound concentration in μM calculated from NMR results, Mass is the peak location, and ID is the proposed identification (a "?" implies uncertainty). "NMR" under "Note" indicates identification in the NMR spectrum, "H_2" implies either H_2 loss or gain from a main peak and may correspond to a radical rearrangement (e.g, Iwahashi et al., 1992), "Org" identifies an organic-P compound. Named compounds are organic-P compounds. These masses are measured to <3 ppm resolution and the masses shown are the theoretical masses consistent with those measured within that 3 ppm error. Nitrogen has been excluded from peak identifications in table 14. NH_4^+ is a relatively inert species acting mostly to preserve charge balance. Despite this, N species may be present at low total concentrations.

additional P compounds were produced, indicating the kinetic stability of these three compounds is higher than phosphite. These stabilities are consistent with those observed by other investigators (Van Wazer, 1958; Schwartz and Van der Veen, 1973).

4. DISCUSSION

We now summarize the salient points of our experimental results with respect to possible reaction pathways. Any proposed reaction pathway should explain these data: (1) The generation of phosphite, orthophosphate, hypophosphate, and pyrophosphate in nearly all phosphide corrosion experiments, (2) the reactivity towards acetate, and the similarity between the H_2O_2 and the acetate phosphide corrosion experiments, (3) the complexity of the mass spectra, (4) the presence of radicals in solution, and (5) the relative stability of the P compounds generated.

The solution chemistry is dominated by phosphite, orthophosphate, hypophosphate, and pyrophosphate. All were detected by NMR and MS of solutions in nearly all phosphide corrosion experiments. All experiments have more phosphite and orthophosphate compared to hypophosphate and pyrophosphate, though exact ratios depend on solution chemistry. MS data reveals complex solution chemistry for high mass species, and detected peroxyphosphates in solution. EPR data suggests that at least two radicals are formed in solution during the corrosion of the phosphide. The peak patterns of these spectra are consistent with the reaction of OH with DMPO to form

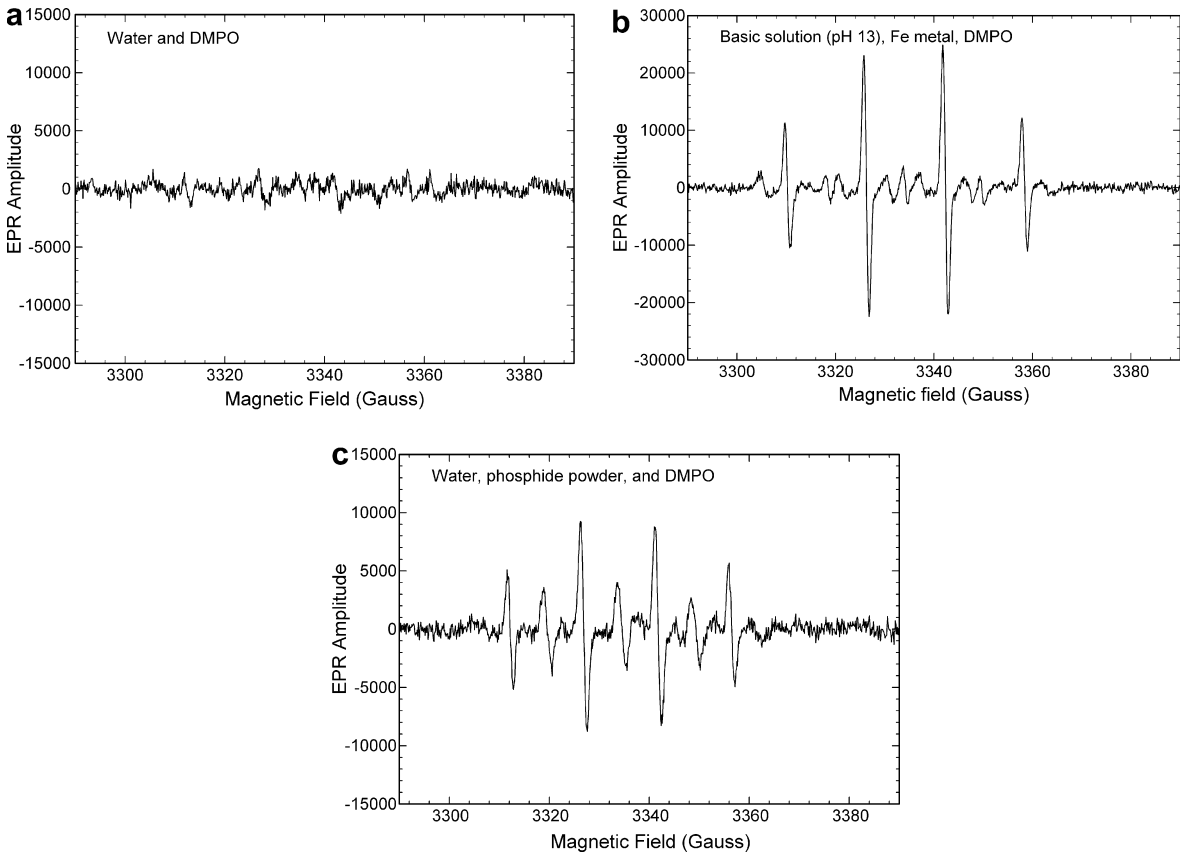

Fig. 4. EPR spectra of solutions.

DMPOOH, and with the reaction of a strong oxidant with DMPO to form DMPOX. The strong oxidant is most likely $\cdot PO_3^{2-}$, as DMPOX is not formed during the corrosion of Fe metal. The DMPOOH radical is also formed during the iron metal powder corrosion.

The most complex spectra result from phosphide corrosion experiments in solutions of H_2O_2 or of sodium acetate. The acetate corrosion solution produced several organic P compounds including acetyl-P compounds and methyl-P compounds, most of which have P–C bonds. A few species have P–O–C bonds similar to those found in modern biochemistry, highlighting the relevance of this study to the origins of life field.

Phosphite, orthophosphate, hypophosphate, and pyrophosphate are all stable in solution in the absence of iron metal powder. Phosphite is oxidized to orthophosphate during the corrosion of iron metal under air. No other P compounds were formed during this corrosion, but $^{\cdot}OH$ radicals were detected in iron corrosion experiments. Hypophosphate and pyrophosphate are both thermodynamically unstable relative to orthophosphate, yet neither compound oxidizes/hydrolyzes to orthophosphate over the timescales of these experiments.

4.1. Other work

The synthesis of hypophosphate by Schwartz and Van der Veen (1973), the synthesis of organic P compounds by de Graaf et al. (1995), and the isotopic work of Bryant and Kee (2006) are relevant to this work. Schwartz and Van der Veen (1973) describe a reaction producing hypophosphate from phosphite in water and in the presence of UV light:

$$2HPO_3^{2-}(aq) \rightarrow P_2O_6^{4-}(aq) + H_2(g) \quad (2)$$

UV light breaks the P–H bond and allows the dimerization of phosphite to form hypophosphate via a phosphite radical.

Following the discovery of phosphonic acids in the Murchison meteorite by Cooper et al. (1992), de Graaf et al. (1995, 1997), and Gorrell et al. (2006) proposed that phosphonic acids may form through a series of radical reactions. The de Graaf et al. (1995) reaction pathway synthesized phosphonic acids through reaction of phosphite with simple organics like formaldehyde under UV light. The Gorrell et al. (2006) model hydrolyzed the compound CP to synthesize phosphonic acids, also through a radical reaction pathway. Both proposed origins of meteoritic phosphonic acids rely on radicals to produce phosphonic acids.

Bryant and Kee (2006) corroded schreibersite in the presence of isotopically labeled $H_2^{18}O$ under air. The resulting NMR splitting patterns suggested that three of the oxygen atoms on phosphite and orthophosphate originated from water, but that one of the oxygen atoms on orthophosphate may have originated from the air. This suggests a common origin for both phosphite and orthophosphate,

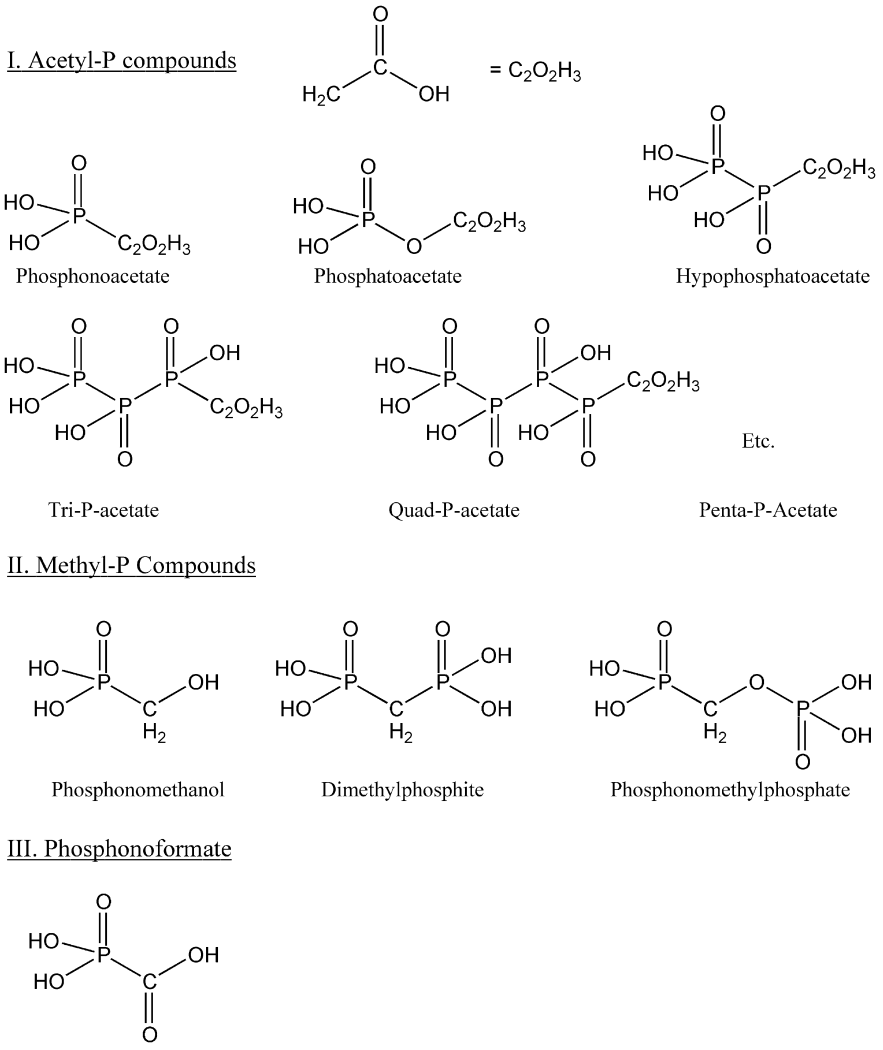

Fig. 5. Structures of organic P compounds produced.

Table 5
Results in terms of percent of total NMR area for P compound stability experiments, Pi is orthophosphate, P3 is phosphite, P4 is hypophosphate, PPi is pyrophosphate, and P1 is hypophosphite

No.	Solution and Material Corroded	Pi (%)	P3 (%)	P4 (%)	PPi (%)	P1 (%)
23	Na_2HPO_3 with Fe	46	54			
24	Na_2HPO_3		100			
25	Na_2HPO_3 with Fe_3O_4		100			
26	NaH_2PO_2 with Fe		25			75
27	NaH_2PO_2		25			75
28	NaH_2PO_2, Na_2HPO_3		52			48
29	NaH_2PO_2, Na_2HPO_3 with Fe_3O_4		70			30
30	Na_2HPO_4 with Fe	100				
31	$Na_4P_2O_6$ with Fe			100		
32	$Na_4P_2O_7$ with Fe				100	

with modification occurring as a secondary step. These data agree with the oxidation of phosphite under air in the presence of iron metal. This transition from H–PO_3 to HO–PO_3 is likely due to a process other than the formation of the initial PO_3 group.

5. PROPOSED REACTION PATHWAY

We propose that the reaction pathway involves the generation, propagation, and recombination of phosphate, phosphite, hydrogen, hydroxyl, and acetate radicals when

acetate is added to solution. These reactions may occur either in solution or on grain surfaces, though both $\cdot PO_3^{2-}$ and OH radicals are present in solution. This reaction pathway provides a pathway to the P salts and to phosphorylated organic compounds.

The EPR data prove the existence of radicals in solution, however, the existence of radicals alone does not imply a radical reaction pathway for the corrosion of schreibersite. The evidence from EPR, NMR, MS, and prior work strongly suggest a radical corrosion pathway when considered together. This is in contrast with an oxidation/reduction model.

Pasek and Lauretta (2005) described a reaction pathway using oxidation/reduction reactions to produce the diversity of P compounds present in solution:

$$Fe_3P + 7H_2O \rightarrow Fe_3O_4 + H_3PO_3 + 5\tfrac{1}{2}H_2(g) \quad (3)$$

$$H_3PO_3 + H_2O \rightarrow H_3PO_4 + H_2(g) \quad (4)$$

$$2H_3PO_3 \rightarrow H_4P_2O_6 + H_2(g) \quad (5)$$

$$H_4P_2O_6 + H_2O \rightarrow H_4P_2O_7 + H_2(g) \quad (6)$$

$$H_4P_2O_7 + H_2O \rightarrow 2H_3PO_4 \quad (7)$$

This proposed reaction pathway was investigated in the series of experiments detailed in the P compound stability experiment section, but did not produce the products predicted. Furthermore, hypophosphate ($P_2O_6^{4-}$) and pyrophosphate ($P_2O_7^{4-}$) are stable and unreactive for the timescales and reaction conditions studied in the experiments described above. Phosphite and iron metal react to form orthophosphate and Fe^{2+}, but this reaction alone is not an oxidation/reduction reaction since no species is reduced. Additionally, the relative concentrations of the various P species are roughly constant even when removed from contact with the powder, which would not be expected if one species turned to another through reaction with water or other P salts. Finally, there is an energetic barrier to the formation of hypophosphate ($\Delta G^\circ = +58$ kJ, pH 7, reaction (5), Gulick, 1955). The active agent leading to hypophosphate must be more energetic than phosphite.

5.1. Generation of radicals

Orthophosphate is the stable form of P in water. Phosphorus in schreibersite exists as oxidation state 0. Thus, the driving force during corrosion of schreibersite is oxidation of P from 0 to +5. We propose that the reaction between water and Fe_3P produces phosphite radicals, and several equivalents of H_2 gas:

$$3Fe_3P + 12H_3O^+ + 2H_2O \rightarrow 5H\cdot + 5\cdot OH + 3\cdot PO_3^{2} + 15H_2 + 9Fe^{2+} \quad (8)$$

Both P and Fe are oxidized in this net reaction. The oxidation state of P changes from 0 to nominally +4 and Fe from 0 to +2. Three radical species are formed: H, OH, and $\cdot PO_3^{2-}$. The production of significant quantities of H_2 gas occurs as the Fe_3P corrodes and is verified by the stoichiometric release of H_2 (see Pasek and Lauretta, 2005). The ratio of phosphite to hydroxyl radicals is derived from the peak heights of the EPR spectrum, and depends on the relative efficiencies of the chemical reactions that form DMPOOH and DMPOX. Hydrogen radicals are hypothesized based on the production of H_2 and phosphite.

Most phosphide corrosion solutions without Mg^{2+} and Ca^{2+} have at least four P species: orthophosphate, pyrophosphate, hypophosphate, and phosphite. The production of three of these P species is readily explained by radical recombination reactions, like the production of phosphite through reaction of a phosphite radical with a hydrogen radical:

$$\cdot PO_3^{2-} + H\cdot \rightarrow HPO_3^{2-} \quad (9)$$

All recombination reactions from the inorganic radical mixture are summarized in a radical matrix (Table 6). The H_2 evolved during corrosion is partly due to a radical recombination of 2H atoms. The production of orthophosphate, hypophosphate, and phosphite is predicted from the initial radical recombination products of schreibersite corrosion.

One of the consequences of this proposed reaction scheme is that orthophosphate and ergo hydroxyl radicals are produced even in anoxic conditions. This is verified by the presence of orthophosphate in all solutions, even those performed under argon. Morton et al. (2003) and Bryant and Kee (2006) reported similar results for corrosion experiments performed under N_2 atmospheres.

Hydrogen peroxide is a predicted product from radical recombination of two hydroxyl radicals. Peroxide forms hydroxyl radicals through reaction with ferrous iron:

$$Fe^{2+} + HOOH \rightarrow Fe(OH)^{2+} + \cdot OH \quad (10)$$

This is the Fenton reaction (Walling, 1976). In most of the inorganic corrosion experiments, this reaction removes all H_2O_2, generating ferric iron and hydroxyl radicals. The net result is that hydrogen peroxide is removed from the system and thus prevented from affecting P chemistry. However, in solutions with significant chelating molecules like acetate, the Fe^{2+} forms organic complexes allowing H_2O_2 to build up and react with the powder and dissolved P species. Thus the addition of excess H_2O_2 in water to Fe_3P produced species similar to the addition of CH_3COO-Na (Fig. 2). Other solutions with chelating agents (like EDTA, pyruvate, and bicarbonate) also have diverse P speciation products.

Table 6
Radical recombination matrix

	$H\cdot$	$\cdot OH$	$\cdot PO_3^{2-}$	$\cdot OPO_3^{2-}$
$H\cdot$	H_2	H_2O	HPO_3^{2-}	HPO_4^{2-}
$\cdot OH$	H_2O	H_2O_2	HPO_4^{2-}	HPO_5^{2-}
$\cdot PO_3^{2-}$	HPO_3^{2-}	HPO_4^{2-}	$P_2O_6^{4-}$	$P_2O_7^{4-}$
$\cdot OPO_3^{2-}$	HPO_4^{2-}	HPO_5^{2-}	$P_2O_7^{4-}$	$P_2O_8^{4-}$

Non-radical species are formed through the recombination of two radical species. The three radicals $H\cdot$, $\cdot OH$, and $\cdot PO_3^{2-}$ can terminate in nine different ways, three of which are redundant. Additional compounds produced if the phosphate radical, $\cdot OPO_3^{2-}$, is added to the radical matrix are shown in the final column and row of this table. All predicted P compounds are observed in the MS data.

Pyrophosphate is a ubiquitous product of all corrosion experiments, but its concentration is the most variable of the four main P species. Pyrophosphate is not predicted as a product resulting from a radical recombination step, given the radicals described in reaction (8). Pyrophosphate is probably formed in a second-generation radical recombination step, like the reaction:

$$\cdot PO_3^{2-} + \cdot OPO_3^{2-} \rightarrow P_2O_7^{4-} \quad (11)$$

This necessitates a source of phosphate ($\cdot OPO_3^{2-}$) radicals. Phosphate radicals could be formed through reaction of orthophosphate and OH or H radicals via a radical propagation reaction:

$$HOPO_3^{2-} + \cdot OH,H\cdot \rightarrow \cdot OPO_3^{2-} + H_2O,H_2 \quad (12)$$

followed by reaction (11). Kinetic studies show these reactions proceed at $\sim 10^5\ M^{-1}s^{-1}$ (Maruthamuthu and Neta, 1978; Buxton et al., 1988). Adding the phosphate radical to the radical matrix (Table 6) provides a pathway to forming a few more P species, including peroxyphosphate and peroxypyrophosphate. Both compounds are observed in the MS analysis.

The mass spectra shown in Fig. 3 and Table 4 demonstrate that there is a huge diversity of P compounds in solution when acetate is added to iron phosphide. Among the diverse chemistry of the P compounds in solution, some are organophosphorus compounds; these are discussed in the next section. The majority are multi-P oxides. How could these compounds form?

Radical reactions lack specificity, and radical reactions frequently produce unusual minor products. These minor products are formed from propagation/recombination steps like reaction of hypophosphate with a radical inducer (like $\cdot PO_3^{2-}$):

$$P_2O_6H_3^- + \cdot PO_3^{2-} \rightarrow \cdot P_2O_5H_3^- + PO_4^{3-} \quad (13)$$

$$\cdot P_2O^5H_3^- + \cdot PO_3^{2-} + H^+ \rightarrow H_4P_3O_8^- \quad (14)$$

This tri-P compound is detected by MS analysis. This process can repeat several times to form species like $H_5P_4O_{10}^-$, $H_6P_5O_{12}^-$, and so on. These reactions occur less and less frequently as the products become rarer and rarer, consistent with the MS analysis.

Fig. 6 summarizes the radical reaction pathway for the inorganic components of the solution. Phosphorus species formed from radical recombinations in turn react with other radicals from the corrosion, resulting in an increasingly complex suite of P compounds. Each cycle or generation has progressively less total abundance for each compound but is more diverse in terms of molecular arrangement. All compounds will eventually oxidize/hydrolyze to the most stable P compound, orthophosphate.

5.2. Proposed organic phosphorus reaction pathway

Acetate is phosphorylated in solution to form a series of P–C and P–O–C linkages. The total yields for organic P compounds are ~3.6% of the total dissolved P compounds.

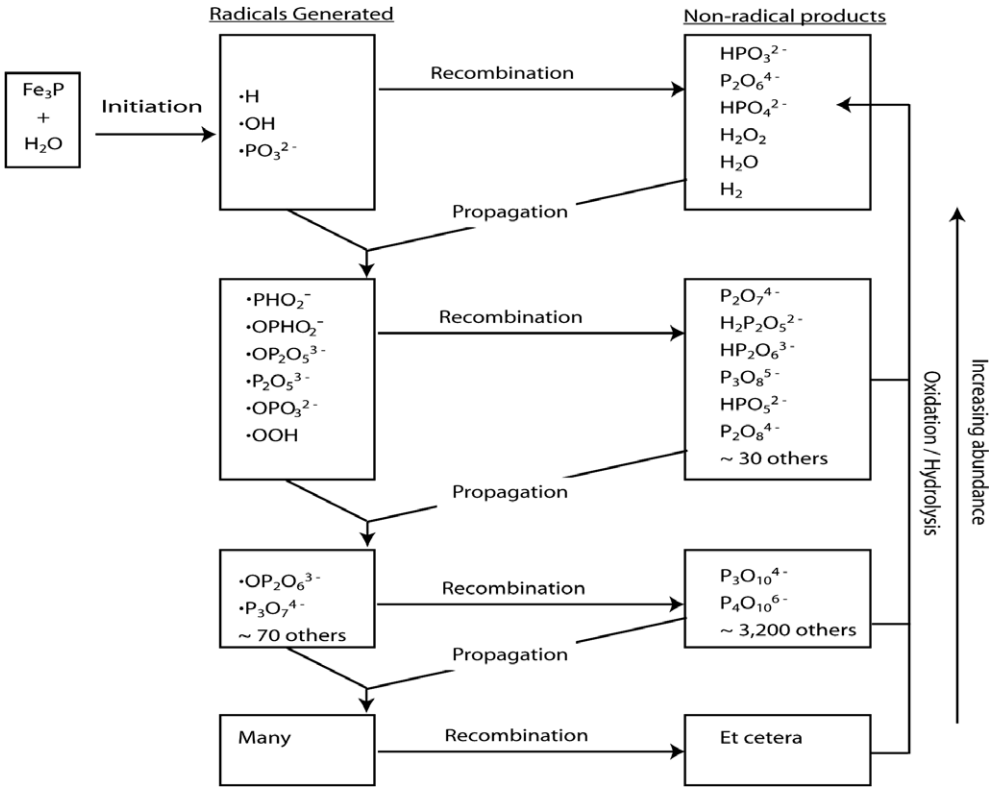

Fig. 6. Proposed inorganic reaction pathway summary.

This yield is consistent with the 0.7% mole fraction of acetate in solution. The phosphorylation products are consistent with the behavior of acetate radicals.

The reaction of acetate with a radical agent forms two distinct radicals: $\cdot CH_2COO^-$ and $CH_3COO\cdot$. The radical CH_3COO is unstable and decarboxylates:

$$CH_3COO\cdot \rightarrow \cdot CH_3 + CO_2 \quad (15)$$

though CO_2 may also form a radical. The $\cdot CH_2COO^-$ radical is comparatively stable (Wang et al., 2001).

The organic P compounds are broadly grouped into three sets: the P-acetyl compounds, the P–CH_2 compounds, and phosphonoformate (Fig. 5). The most abundant species are the ones with the lowest molecular weight, consistent with relative concentrations of radical species. P-acetyl compounds are formed through radical recombination reactions between the inorganic radicals resulting from corrosion described in Section 5.1 and the stable acetate radical described above. The P–CH_2 compounds may be formed through a decarboxylation reaction of acetyl phosphonate:

$$O_3PCH_2COO^{3-} + \cdot OH \rightarrow O_3PCH_2COO\cdot 2- + OH^- \rightarrow O_3PCH_2\cdot 2- + HCO_3^- \quad (16)$$

followed by a recombination reaction to form a new group of organic P compounds (Fig. 7). Alternatively, the CO_2 can retain the free radical and react with a phosphite radical to form phosphonoformate:

$$O_3PCH_2COO\cdot^{2-} \rightarrow O_3PCH_2^- + \cdot CO_2^- \rightarrow \cdot CO_2^- + \cdot PO_3^{2-} \rightarrow O_2CPO_3^{3-} \quad (17)$$

Only acetate and pyruvate appear to react with the corroding phosphide powder to produce organic P compounds, whereas ethanol and acetonitrile were not phosphorylated. The glycolaldehyde and acetone solutions turned to tar in corroding solutions and could not be analyzed. Acetate, EDTA, pyruvate, glycolaldehyde, acetone, and acetaldehyde are capable of a keto-enol tautomerization transformation whereas neither ethanol nor acetonitrile tautomerize. Keto-enol tautomerization increases the acidity of protons on α carbons next to carbonyl groups and stabilizes radicals. Acetate has a charged functional group at a pH of 7 which repels other acetate groups, limiting polymerization. Glycolaldehyde and acetone lack negative charges and hence both polymerized to form tar.

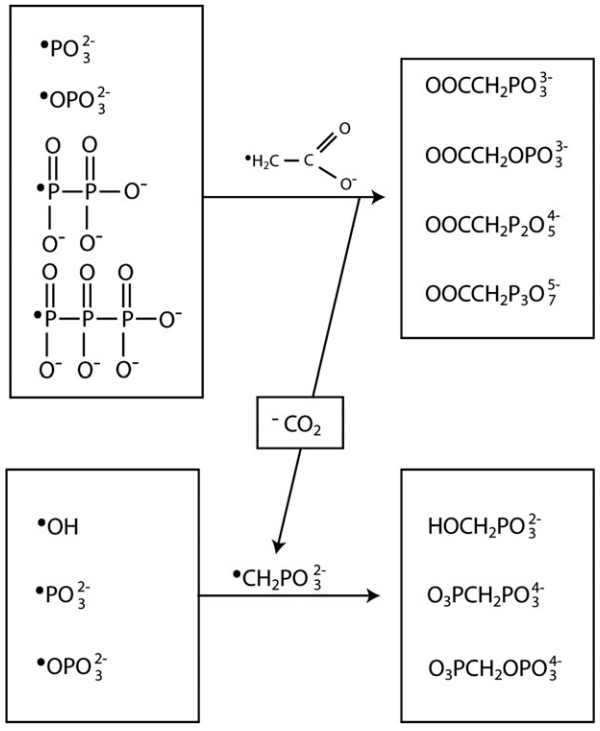

Fig. 7. Proposed organic P reaction pathway summary.

EDTA forms similar radicals, losing an H from the methyl bridge but the concentration of EDTA (0.025 M) used in these experiments was much lower than the concentration of acetate (0.4 M), so organic P compounds were more difficult to detect in those solutions. Acetaldehyde lacks a negative charge, but acetaldehyde oxidizes to acetate in the presence of Fe^{3+}, and it is reaction of P radicals with this acetate that is being detected instead of reaction with acetaldehyde.

5.3. Phosphite oxidation and isotopic evidence

Fig. 4b demonstrates that OH radicals are produced during the corrosion of iron metal. These OH radicals are produced through reaction of O_2 gas with the iron metal:

$$Fe + O_2 \rightarrow Fe^{2+} + O_2^{2-} \quad (18)$$

$$O_2^{2-} + 2H^+ \rightarrow H_2O_2 \quad (19)$$

$$Fe^{2+} + H_2O_2 \rightarrow Fe(OH)^{2+} + \cdot OH \quad (10)$$

An analogous reaction is known for cobalt (Leonard et al., 1998). To the best of our knowledge, this is the first detection of ·OH radical production from the corrosion of iron metal.

The detection of OH radicals is coupled to the phosphite oxidation experiment results (see Section 3.5). Phosphite is oxidized by OH radicals produced during the corrosion of iron in this experiment through a radical propagation reaction:

$$HPO_3^{2-} + \cdot OH \rightarrow \cdot PO_3^{2-} + H_2O \quad (20)$$

$$\cdot PO_3^{2} + \cdot OH \rightarrow HOPO_3^{2-} \quad (21)$$

This experiment demonstrates that the conversion of phosphite to orthophosphate occurs through radical reactions.

The results above match well with the isotopic data accumulated by Bryant and Kee (2006), who state that three of the oxygen atoms share the same origin for both phosphite and orthophosphate. The origin of these three oxygen atoms is the water corroding the schreibersite. The results above provide evidence that the change from phosphite to orthophosphate is promulgated by radicals from O_2 corroding iron.

6. CONCLUSION

Phosphide corrodes in water to form three major species—hydroxyl, hydrogen, and phosphite radicals. The

recombination of these three radicals produces the orthophosphate, phosphite, and hypophosphate species. Secondary radical propagation reactions produce pyrophosphate and many minor P species. Interactions of these radicals with organic radicals in turn forms organophosphorus compounds, with P–C and P–O–C linkages.

The P products are most likely produced through radical recombination reactions. They may be removed through oxidation, hydrolysis, or radical propagation reactions. Radical reactions are faster than oxidation or hydrolysis reactions due to the vast difference in energy between the reaction intermediates and products for radical reactions. Thus the suite of P species is the most complex while the phosphide corrodes. After all the phosphide has corroded the P compounds will oxidize to form orthophosphate. The C–P and the P–P bonds are among the strongest bonds present, and may not be broken except on geologic timescales. The final products predicted from the long timescale of corrosion are orthophosphate with some C–P and P–P compounds. C–P compounds are well known in meteorites (Cooper et al., 1992), but P–P linkages are not. The detection of parts per thousand (with respect to total P) hypophosphate concentrations in meteorites would provide evidence for schreibersite corrosion acting on the parent bodies of meteorites. Unfortunately, hypophosphate is the least soluble of the four major inorganic P compounds, and its detection may be difficult.

The P speciation products in these reaction systems are independent of atmosphere (Ar or air). The major effect of changing the atmosphere above the experiments appears to be total yield of P compounds. The relative yields of specific P species do not appear to depend on the atmosphere. We speculate that this is due to the ability of Fe (as Fe_3P) to remove O_2 from the water. The oxidation of Fe to Fe^{2+} and Fe^{3+} helps break down the Fe_3P, increasing available reactive surface area, and thus increasing yield. The O_2 from the air is in turn reduced to OH^- which readily reacts with Fe^{3+} to form the reddish brown Fe-OH compounds reported in the experiments done under air. The net effect of performing these experiments under air is an increase in yield of P compounds with little effect on P speciation.

6.1. Implications for the origin of life

Inorganic phosphates or polyphosphates have long been thought to be the most important source of phosphate for prebiotic synthesis, although reduced forms have occasionally been considered in this context (Schwartz, 1997; Peyser and Ferris, 2001; de Graaf and Schwartz, 2005). Only orthophosphates are abundant in terrestrial rocks, principally calcium phosphate. As a result, numerous approaches to prebiotic synthesis using inorganic orthophosphates or polyphosphates have been explored.

Many of the early attempts to phosphorylate nucleosides used condensing agents such as cyanamide or cyanate. Unfortunately, such reactions are inefficient in aqueous solutions because water competes for the activated phosphate intermediate (Lohrmann and Orgel, 1968). More recently it has been shown that AMP can be converted to ADP and ATP by cyanate in the presence of insoluble calcium phosphates (Yamagata, 1999), though the initial phosphorylation to AMP is still unclear.

Despite its importance to biology and intense research, the mechanism by which P was incorporated into biomolecules is still unknown (Schwartz, 1997). With the exception of apatite, none of the inorganic P sources used in successful phosphorylation experiments occur in abundance in natural systems. Polyphosphates are produced through heating in μM quantities (Yamagata et al., 1991), with phosphorylation yields of ~1% (Schwartz and Ponnamperuma, 1968) for a total organophosphate concentration of $\sim 10^{-8}$ M, too low for most origin of life scenarios.

Radical recombination reactions overcome the energetic difficulties traditionally associated with origin of life studies. The reaction of a P radical with an organic radical or organic compound produces an organic P compound without the need for condensing agents, elevated temperatures, or geologically rare P compounds. Recognizing these benefits, other researchers have used radical reactions to produce organophosphates (e.g., Simakov and Kuzicheva, 2005).

Organic P compounds produced during schreibersite corrosion have P–C and P–O–C linkages. Phosphonates have P–C linkages and are ubiquitous in biochemistry, especially lipids (Kononova and Nesmeyanova, 2002), though little is known of their exact biochemical function (Hilderbrand and Henderson, 1983). As a testament to their ubiquity, approximately 25% of all marine dissolved organic P is phosphonates (Kolowith et al., 2001; Paytan et al., 2003). The formation of the critical P–O–C linkage via simple schreibersite corrosion emphasizes the role that meteorites may have played in the "priming" of the early Earth with organic P compounds.

The total yield of P–O–C type compounds is approximately 1% of the total soluble P compounds produced. This yield is roughly proportional to the mole fraction of organic compounds in solution. The thermodynamic instability of schreibersite will result in complete corrosion of this mineral with time, and the total yield of organophosphates from schreibersite will approach 1% of the total P. The main organophosphate produced is phosphoglyocolate, which is minor byproduct in modern metabolism, but the production of this compound indicates that changing the initial conditions or varying the organic chemistry may produce critical P–O–C compounds.

Additionally, this work provides a pathway to the inorganic production of pyrophosphate. Pyrophosphate could have preceded ATP as the metabolic energy carrier for life (Baltscheffsky, 1993; Baltscheffsky, 1997; Baltscheffsky et al., 1997). Archaea and some extremophiles employ pyrophosphate as a substitute for ATP for several metabolic reactions (Serrano et al., 2004), suggesting an ancient role in metabolism for this molecule.

Schreibersite is a ubiquitous mineral in many meteorites, especially the iron meteorites. Iron meteorites are the main component of massive meteorite falls (10^3–10^{10} kg, see Bland and Artemieva, 2006) and during the late heavy bombardment, could have deposited between 10^6 and 10^{10} kg of phosphorus as reactive schreibersite across the surface of the Earth per year (Pasek, 2006). Using the yields from the acetate experiments, this would correspond to a

production rate of 10^5–10^8 kg of organophosphate compounds per year through schreibersite corrosion and an equivalent production of pyrophosphate and polyphosphates per year.

The formation of craters by meteorite impacts provides a plausible geomorphologic process that concentrated reactive P for reaction with organic compounds. Iron meteorites form most of the small craters (<10 km diameter) on the surface of the Earth (Bland and Artemieva, 2006), and these craters often have associated crater-lakes at their topographic lows. On the early Earth slope runoff and drying cycles concentrated soluble organics produced by endogenous processes (cf., Cockell, 2006) or delivered from exogenous sources to concentrations between 1.0 and 0.001 M, depending on the endogenous production rate (Pasek, 2006). Using the Murchison chondrite as a proxy to estimate the composition of the organic inventory, a majority of this material would be carboxylic acids (Pizzarello et al., 2006) which are demonstrated to react with schreibersite at a yield proportionate to the mole fraction. These organics could react with the several tons of meteoritic material at the bottom of the crater to produce organophosphates (10^{-2}–10^{-5} M) and other important prebiotic compounds.

This study provides the results of a series of experiments and analyses of synthetic schreibersite corrosion. It demonstrates that schreibersite most likely corrodes by a radical reaction pathway, and that radicals are capable of overcoming energetic barriers traditionally associated with the prebiotic synthesis of organic P compounds. As such, it provides strong evidence that meteorites may have been critical to the development of life on the Earth.

ACKNOWLEDGMENTS

We thank S. Benner, G. Cody, and three anonymous reviewers for helpful discussions. This work was supported by NASA Exobiology, grant NAG5-13470 (D.S.L.), and by the NASA Astrobiology Institute and the Goddard Center for Astrobiology (J.P.D.), and through a GSRP grant through the NASA Astrobiology Institute and the Goddard Center for Astrobiology (M.A.P.). We also thank Joseph A. Nuth III, James H. Doty III, and Andrei Astashkin for technical assistance.

REFERENCES

Baltscheffsky H. (1993) Chemical origin and early evolution of biological energy conversion. In *Chemical Evolution: Origin of Life* (eds. C. Ponnamperuma and J. Chela-Flores). A Deepak Publication, Hampton, pp. 13–23.

Baltscheffsky H. (1997) Major "anastrophes" in the origin and early evolution of biological energy conversion. *J. Theor. Biol.* **187**, 495–501.

Baltscheffsky H., Blomberg C., Liljenstrom H., Lindahl B. I. B., and Arhem P. (1997) On the origin and evolution of life: An introduction. *J. Theor. Biol.* **187**, 453–459.

Bland P. A., and Artemieva N. A. (2006) The rate of small impacts on Earth. *Meteorit. Planet. Sci.* **41**, 607–632.

Bryant D. E., and Kee T. P. (2006) Direct evidence for the availability of reactive, water soluble phosphorus on the early Earth. H-Phosphinic acid from the Nantan meteorite. *Chem. Commun.* **2006**, 2344–2346.

Buxton G. V., Greenstock C. L., Helman W. P., and Ross A. B. (1988) Critical review of rate constants for reactions of hydrated electrons, hydrogen atoms, and hydroxyl radicals (OH/O^-) in aqueous solution. *J. Phys. Chem. Ref. Data* **17**, 513–886.

Cockell C. S. (2006) The origin and emergence of life under impact bombardment. *Phil. Trans. Royal Soc. B* **361**, 1845–1856.

Cooper G. W., Onwo W. M., and Cronin J. R. (1992) Alkyl phosphonic-acids and sulfonic-acids in the Murchison meteorite. *Geochim. Cosmochim. Acta* **56**, 4109–4115.

de Graaf R. M., and Schwartz A. W. (2005) Thermal synthesis of nucleoside H-phosphonates under mild conditions. *Origins Life Evol. B.* **35**, 1–10.

de Graaf R. M., Visscher J., and Schwartz A. W. (1995) A plausibly prebiotic synthesis of phosphonic acids. *Nature* **378**, 474–477.

de Graaf R. M., Visscher J., and Schwartz A. W. (1997) Reactive phosphonic acids as prebiotic carriers of phosphorus. *J. Mol. Evol.* **44**, 237–241.

Gorrell I. B., Wang L., Marks A. J., Bryant D. E., Bouillot F., Goddard A., Heard D. E., and Kee T. P. (2006) On the origin of the Murchison meteorite phosphonates. Implications for prebiotic chemistry. *Chem. Commun.* **2006**, 1643–1645.

Gulick A. (1955) Phosphorus as a factor in the origin of life. *Am. Sci.* **43**, 479–489.

Hilderbrand R. L., and Henderson T. O. (1983) Phosphonic acids in nature. In *The Role of Phosphonates in Living Systems* (ed. R.L. Hilderbrand). CRC Press, Boca Raton, pp. 5–30.

Iwahashi H., Parker C. E., Mason R. P., and Tomer K. B. (1992) Combined liquid chromatography/electron paramagnetic resonance spectrometry/electrospray ionization mass spectrometry for radical identification. *Anal. Chem.* **62**, 2244–2252.

Keefe A. D., and Miller S. L. (1995) Are polyphosphates or phosphate esters pre-biotic reagents? *J. Mol. Evol.* **41**, 693–702.

Kolowith L. C., Ingall E. D., and Benner R. (2001) Composition and cycling of marine organic phosphorus. *Limnol. Oceanogr.* **46**, 309–320.

Kononova S. V., and Nesmeyanova M. A. (2002) Phosphonates and their degradation by microorganisms. *Biochemistry (Moscow)* **67**, 220–233.

Leonard S., Gannett P. M., Rojanasakul Y., Schwegler-Berry D., Castranova V., Vallyathan V., and Shi X. (1998) Cobalt-mediated generation of reactive oxygen species and its possible mechanism. *J. Inorg. Biochem.* **70**, 239–244.

Lohrmann R., and Orgel L. E. (1968) Prebiotic synthesis: phosphorylation in aqueous solution. *Science* **171**, 64–66.

Macià E., Hernández M. V., and Oró J. (1997) Primary sources of phosphorus and phosphates in chemical evolution. *Origins Life Evol. B.* **27**, 459–480.

Maruthamuthu P., and Neta P. (1978) Phosphate radicals. Spectra, acid-base equilibria, and reactions with inorganic compounds. *J. Phys. Chem.* **82**, 710–713.

Morton S. C., Glindemann D., and Edwards M. A. (2003) Phosphates, phosphites, and phosphides in environmental samples. *Environ. Sci. Technol.* **37**, 1169–1174.

Noguchi Y., Nakai Y., Shimba N., Toyosaki H., Kawahara Y., Sugimoto S., and Suzuki E. (2004) The energetic conversion competence of *Escherichia coli* during aerobic respiration studied by ^{31}P NMR using a circulating fermentation system. *J. Biochem.* **136**, 509–515.

Ozawa T., and Hanaki A. (1987) Spin-trapping of phosphorus-containing inorganic radicals by a water-soluble spin-trap, 3,5-dibromo-4-nitrosobenzenesulfonate. *Chem. Lett.* **1987**, 1885–1888.

Ozawa T., and Hanaki A. (1989) Spin trapping of short-lived phosphorus-containing inorganic radicals. *Nippon Kagaku Kaishi* **8**, 1408–1411.

Pasek, M. A. 2006. Phosphorus and sulfur cosmochemistry: implications for the origins of life. Ph.D. Thesis, University of Arizona.

Pasek M. A., and Lauretta D. S. (2005) Aqueous corrosion of phosphide minerals from iron meteorites: a highly reactive source of prebiotic phosphorus on the surface of the early Earth. *Astrobiology* **5**, 515–535.

Paytan A., Cade-Menun B. J., McLaughlin K., and Faul K. L. (2003) Selective phosphorus regeneration of sinking marine particles: evidence from ^{31}P NMR. *Mar. Chem.* **82**, 55–70.

Peyser J. R., and Ferris J. P. (2001) The rates of hydrolysis of thymidyl-3',5'-thymidine-H-phosphonate: The possible role of nucleic acids linked by diesters of phosphorous acid in the origins of life. *Origins Life Evol. B.* **31**, 363–380.

Pizzarello S., Cooper G. W., and Flynn G. J. (2006) The nature and distribution of the organic material in carbonaceous chondrites and interplanetary dust particles. In *Meteorites and the Early Solar System II* (eds. D.S. Lauretta and H.Y. McSween). University of Arizona Press, Tucson, pp. 625–651.

Robitaille P.-M. L., Robitaille P. A., Brown, Jr., G. G., and Brown G. G. (1991) An analysis of the pH-dependent chemical-shift behavior of phosphorus-containing metabolites. *J. Magn. Reson.* **92**, 73–84.

Sankarapandi S., and Zweier J. L. (1999) Evidence against the generation of free hydroxyl radicals from the interaction of copper, zinc-superoxide dismutase and hydrogen peroxide. *J. Biol. Chem.* **274**, 34576–34583.

Satre M., Martin J.-B., and Klein G. (1989) Methyl phosphonate as a ^{31}P-NMR probe for intracellular pH measurements in Dictyostelium amoebae. *Biochimie* **71**, 941–948.

Schwartz A. W. (1997) Prebiotic phosphorus chemistry reconsidered. *Origins Life Evol. B.* **27**, 505–512.

Schwartz A. W., and Ponnamperuma C. (1968) Phosphorylation on the primitive earth. Phosphorylation of adenosine with linear polyhosphate salts in aqueous solution. *Nature* **218**, 443.

Schwartz A. W., and Van der Veen M. (1973) Synthesis of hypophosphate by ultraviolet irradiation of phosphite solutions. *Inorg. Nucl. Chem. Lett.* **9**, 39–41.

Serrano A., Perez-Castineira J. R., Baltscheffsky H., and Baltscheffsky M. (2004) Proton-pumping inorganic pyrophosphatases in some archaea and other extremophilic prokaryotes. *J. Bioenerg. Biomembr.* **3**, 127–133.

Simakov M. B., and Kuzicheva E. A. (2005) Abiotic photochemical synthesis on surface of meteorites and other small bodies. *Adv. Space Res.* **36**, 190–194.

Van Wazer J. R. (1958) Phosphorous and Its Compounds. vol. 1. Interscience, New York.

Wang W. F., Schuchmann M. N., Schuchmann H. P., and von Sonntag C. (2001) The importance of mesomerism in the termination of α-carboxymethyl radicals from aqueous malonic and acetic acids. *Chem. Eur. J.* **7**, 791–795.

Walling C. (1976) Fenton's reagent revisited. *Acc. Chem. Res.* **8**, 125–131.

Yamagata Y. (1999) Prebiotic formation of ADP and ATP from AMP, calcium phosphates and cyanate in aqueous solution. *Origins Life Evol. B.* **29**, 511–520.

Yamagata Y., Watanabe H., Saitoh M., and Namba T. (1991) Volcanic production of polyphosphates and its relevance to prebiotic evolution. *Nature* **352**, 516–519.

Yoza N., and Ohashi S. (1965) Oxidation of red phosphorus with hydrogen peroxide and isolation of disodium dihydrogen hypophosphate. *Bull. Chem. Soc. Japan* **38**, 1408–1409.

Yoza N., Ueda N., and Nakashima S. (1994) pH-dependence of P-31-NMR spectroscopic parameters of monofluorophosphate, phosphate, hypophosphate, phosphonate, phosphinate and their dimers and trimers. *Fresen. J. Anal. Chem.* **348**, 633–638.

Associate editor: Johnson R. Haas